

# DROP: Distributional and Regular Optimism and Pessimism for Reinforcement Learning

Taisuke Kobayashi\*

Dr. T. Kobayashi

National Institute of Informatics (NII) and The Graduate University for Advanced Studies (SOK-ENDAI), Tokyo, Japan

Email Address: kobayashi@nii.ac.jp

URL: <https://prinlab.org/en/>

Keywords: *Distributional reinforcement learning, Control as inference, Optimism and pessimism, Ensemble model*

In reinforcement learning (RL), temporal difference (TD) error is known to be related to the firing rate of dopamine neurons. It has been observed that each dopamine neuron does not behave uniformly, but each responds to the TD error in an optimistic or pessimistic manner, interpreted as a kind of distributional RL. To explain such a biological data, a heuristic model has also been designed with learning rates asymmetric for the positive and negative TD errors. However, this heuristic model is not theoretically-grounded and unknown whether it can work as a RL algorithm. This paper therefore introduces a novel theoretically-grounded model with optimism and pessimism, which is derived from control as inference. In combination with ensemble learning, a distributional value function as a critic is estimated from regularly introduced optimism and pessimism. Based on its central value, a policy in an actor is improved. This proposed algorithm, so-called DROP (distributional and regular optimism and pessimism), is compared on dynamic tasks. Although the heuristic model showed poor learning performance, DROP showed excellent one in all tasks with high generality. In other words, it was suggested that DROP is a new model that can elicit the potential contributions of optimism and pessimism.

## 1 Introduction

Among the machine learning technologies that have made dramatic progress in recent years, reinforcement learning (RL) [1] stands out for its uniqueness. RL, which was developed and established in the context of optimal control, has begun to be used in a wide range of fields: such as robotics [2]; game AI [3]; and autonomous driving [4]. On the other hand, RL deals with decision-making problems that consider the agent's future, and analogies with those of animals (including human) have been pointed out. Based on that, various research groups have found several correspondences between the decision-making data of animals and RL or its components, as exemplified below:

- The temporal difference (TD) error in RL is proportional to the firing rate of dopamine neurons [5, 6].
- The discount factor in RL, i.e. how far into the future to be considered, is related to the amount of serotonin [7, 8].
- The intrinsic motivation manipulates the external rewards in RL, making human adapt to various situations [9, 10].
- The perceptual and value-based decision making is in the duality according to control as inference [11], and it might be implemented on the sensory and motor cortical circuits [12].

Conversely, RL algorithms inspired by biological decision-making mechanisms have also been developed, improving RL performance from various perspectives with the following examples:

- The biological Levy walk was conceptually introduced into the exploration strategy in RL, improving sample efficiency of optimization [13, 14].
- The extended RL framework, which reflects the fact that different information processing is conducted in reward and punishment, improved the performance of safely finding the optimal solution [15, 16].

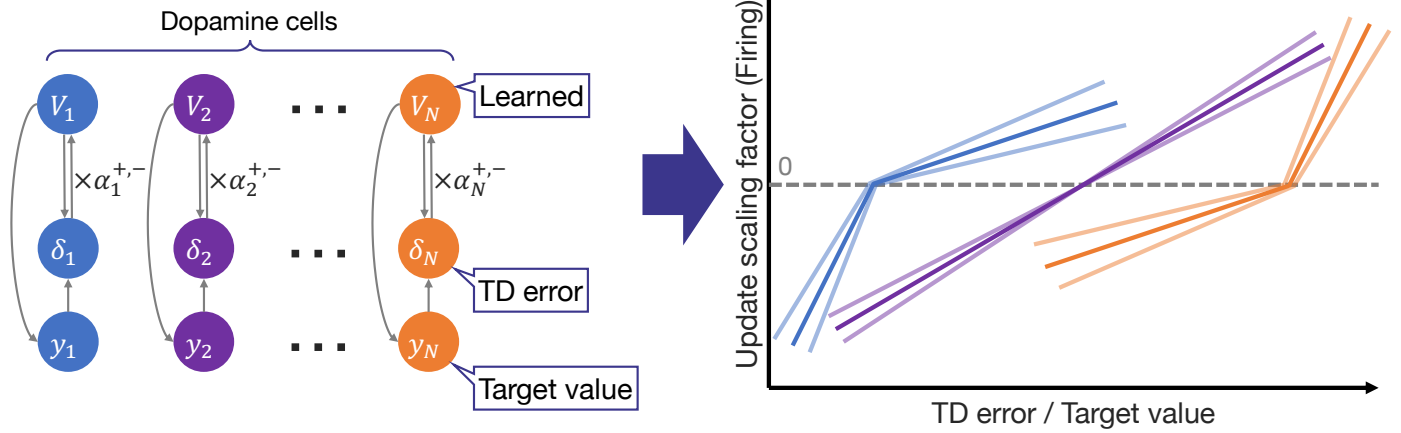


Figure 1: Heuristic model designed in the previous studies [18, 19]: because the model is an ensemble model with each dopamine neuron estimating its value function individually, the origin at which the TD error becomes zero is different for each neuron; each neuron has an asymmetric learning rate depending on the sign of TD error, so that some neurons learn optimistically, preferring a better outcome than predicted, while others are pessimistic for preferring a worse outcome than predicted.

- The world model, which subjectively represents the state in RL according to the agent's observation, allows the agent to simulate the interaction with environment, facilitating learning and/or avoiding risky behaviors in real world [2, 17].

Thus, RL is studied more deeply both in terms of understanding the decision-making models of animals and implementing them as learning algorithms.

Among them, this paper focuses on the latest studies on TD errors and the firing of dopamine neurons [18, 19]. In these papers, it is reported that dopamine neurons fire at different times. This suggests that each dopamine neuron independently learns its own value function that minimizes the corresponding TD error, and that decisions are made by combining these value functions. Furthermore, some dopamine neurons have asymmetrically biased firing patterns depending on the positive or negative TD error, leading to the distributional estimation of the value function as the distributional RL [20, 21]. To represent these characteristics, a heuristic model was introduced in which the learning rate  $\alpha$  is asymmetrically given for the positive and negative TD errors, as shown in Fig. 1.

This asymmetric learning rate brings optimism and pessimism to RL, which are well known to be useful in RL algorithms. Optimism can be incorporated into efficient exploration methods because it encourages the acquisition of diverse experiences without fear of the unknown states [22]. Pessimism, on the other hand, is sensitive to risk and is an important concept in safety-oriented methods [23]. Since each has its own advantages and disadvantages, the complementary combination of these two has been studied actively [24–26].

The above heuristic model, which should represent both optimism and pessimism, seems to be useful enough as an RL algorithm. Intuitively, however, there is a concern that it may destabilize RL because of the unsmoothness in the update amounts based on TD errors. We should derive and verify a model with optimism and pessimism that is more theoretically plausible as a RL algorithm.

Therefore, this paper focuses on the previous work [27]. In this paper, the learning rule for value and policy functions in RL is rederived based on the concept of control as inference [11]. In other words, the problem setting of RL is changed from maximizing the cumulative rewards in the future to optimizing the probability of optimality defined by them, and the approximated gradients for the new problem setting are shown to be consistent with the conventional learning rule. By revisiting the arbitrary definitions behind this problem setting, a theoretically-grounded optimistic learning rule can be derived with its parameterization, enabling as an RL algorithm to accelerate exploration.

Based on this previous work, the first objective of this paper is to find a new derivation method, which converts the optimism derived into pessimism in a similar way. For this purpose, the original definition

of optimality used in the derivation of optimism is modified to its inversion. Afterward, using the same procedure of computing the approximated gradients as in the previous study, the pessimistic learning rule is parameterized as well. It is also pointed out that these optimism and pessimism can be expressed and adjusted with a single parameter by integrating their learning rules.

Next, a RL algorithm to learn all components of an ensemble model for representing the value function with different optimistic and pessimistic parameters, respectively. However, since the parameter is defined in real space, it is difficult to place multiple parameters such that their optimism and/or pessimism effectively exerted should be regularly distributed. Based on the boundedness of the nonlinear (i.e. optimistic or pessimistic) TD errors, the original parameter is invertibly transformed to bounded one, which can intuitively be spaced on its bounded space. By interpreting the obtained value functions as a multi-objective optimization problem, policy improvement is implemented based on the median of nonlinear TD errors.

The developed RL algorithm, so-called DROP (distributional and regular optimism and pessimism), is compared with the heuristic model in the previous studies [18, 19] and benchmark performance using two dynamics simulators [28, 29]. The results show that the heuristic model destabilizes learning by failing to properly converge the TD error of the pessimistic value function. In contrast, DROP succeeds in learning efficiently and stably in all benchmark tasks to a level where the tasks could qualitatively be considered successful.

## 2 Preliminaries

### 2.1 Reinforcement learning

RL aims to optimize a policy of a learnable agent so that the accumulation of future rewards from an unknown environment (so-called return) is maximized [1]. This problem assumes Markov decision process (MDP) with the tuple  $(\mathcal{S}, \mathcal{A}, \mathcal{R}, p_0, p_e)$ . Specifically, the state  $s \in \mathcal{S}$  is sampled from the environment with either of probabilities,  $s \sim p_0(s)$  as the initial random state or  $s \leftarrow s' \sim p_e(s' | s, a)$  as the state transition. The agent decides the action  $a \in \mathcal{A}$  according to  $s$ , using the policy  $a \sim \pi(a | s)$ , which can be learned by updating its parameters  $\phi$ .  $a$  yields the state transition  $s' \sim p_e(s' | s, a)$ , and then, this one step is evaluated as the reward  $r = r(s, a) \in \mathcal{R}$ .

By sequentially repeating the above step with the experience data  $(s, a, s', r)$ , the agent obtains the following return  $R_t$  from the current time step  $t$ .

$$R_t = \sum_{k=0}^{\infty} \gamma^k r_{t+k} \quad (1)$$

where  $\gamma \in [0, 1)$  denotes the discount factor.

Under this MDP,  $\pi(a | s)$  is optimized as follows:

$$\pi^*(a | s) = \arg \max_{\pi} \mathbb{E}_{p_e, \pi}[R_t | s_t = s] \quad (2)$$

Note that  $\mathbb{E}_{p_e, \pi}[R_t | s_t = s]$  is defined as the (state) value function  $V(s)$ , which is approximated with its parameters  $\theta$ .

### 2.2 Optimism from control as inference

In the previous work, a theoretically-grounded optimistic RL has been derived [27]. Following it, this paper introduces a stochastic variable for optimality,  $O = \{0, 1\}$ , which is relevant to the return. The conditional probability of  $O = 1$  (i.e. the future is optimal) is modeled with  $\beta \in \mathbb{R}_+$  the inverse temperature parameter.

$$p(O = 1 | s) = e^{\beta(V(s) - \bar{R})} \quad (3)$$

$$p(O = 1 | s, a) = e^{\beta(Q(s, a) - \bar{R})} \quad (4)$$

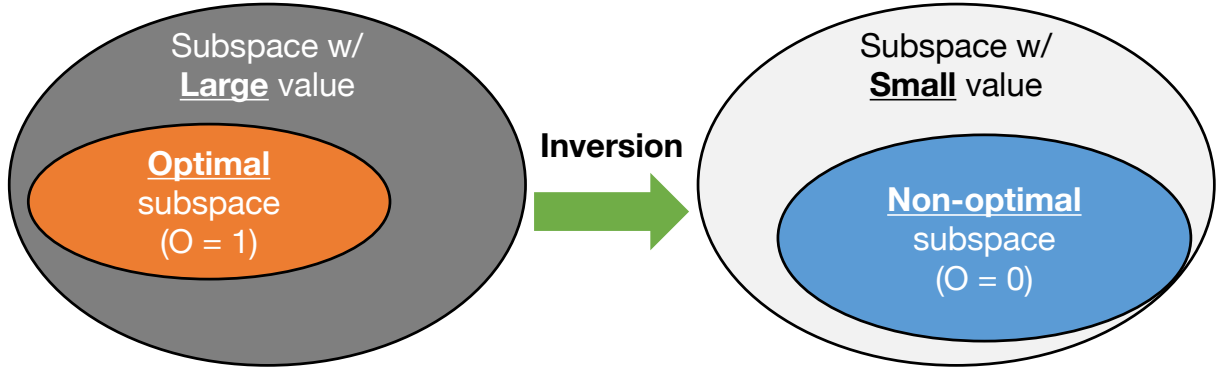


Figure 2: Inversion of the definition of optimality: the definition of optimality in the previous studies [11, 27] was that the larger the value function, the more optimal (i.e.  $O = 1$ ) it is, as shown on the left side; the inversion is similar but different that the smaller the value function, the more non-optimal (i.e.  $O = 0$ ) it is, as shown on the right side.

where  $Q(s, a) = \mathbb{E}_{p_e, \pi}[R_t \mid s_t = s, a_t = a]$  denotes the action value function and can be approximated to be  $r + \gamma V(s')$  according to Bellman equation.  $\bar{R}$  is the implicit maximum return to satisfy  $p(O = 1) \in (0, 1)$ . Note that the probability of  $O = 0$  can be easily given as  $O$  is binary.

Here, the optimal and non-optimal policies can be theoretically inferred (although they cannot be directly used for generating  $a$ ). Specifically, with the baseline policy  $b(a \mid s)$  for sampling actions,  $\pi(a \mid s, O)$  is given according to Bayesian theorem as follows:

$$\begin{aligned} \pi(a \mid s, O) &= \frac{p(O \mid s, a)b(a \mid s)}{p(O \mid s)} \\ &= \begin{cases} \frac{e^{\beta(Q(s, a) - \bar{R})}}{e^{\beta(V(s) - \bar{R})}} b(a \mid s) =: \pi^+(a \mid s) & O = 1 \\ \frac{1 - e^{\beta(Q(s, a) - \bar{R})}}{1 - e^{\beta(V(s) - \bar{R})}} b(a \mid s) =: \pi^-(a \mid s) & O = 0 \end{cases} \end{aligned} \quad (5)$$

Under the above setup, the following two optimization problems with Kullback-Leibler (KL) divergences are solved.

$$\min_{\theta} \mathbb{E}_{p_e, b}[\text{KL}(p(O \mid s, a) \mid p(O \mid s))] \quad (6)$$

$$\min_{\phi} \mathbb{E}_{p_e}[\text{KL}(\pi^+(a \mid s) \mid \pi(a \mid s)) - \text{KL}(\pi^-(a \mid s) \mid \pi(a \mid s))] \quad (7)$$

where  $\text{KL}(p_1 \mid p_2) = \mathbb{E}_{x \sim p_1}[\ln p_1(x) - \ln p_2(x)]$ .

The approximated gradients for solving these are derived below (for detailed derivation processes, see the literature [27] and the derivation process for the pessimistic RL in the next section).

$$g_{\theta}^{\text{optim}} = \mathbb{E}_{p_e, b}[-\beta^{-1}(e^{\beta(r + \gamma V(s') - V(s))} - 1) \nabla_{\theta} V(s)] \quad (8)$$

$$g_{\phi}^{\text{optim}} = \mathbb{E}_{p_e, b}[-\beta^{-1}(e^{\beta(r + \gamma V(s') - V(s))} - 1) \nabla_{\phi} \ln \pi(a \mid s)] \quad (9)$$

As  $r + \gamma V(s') - V(s)$  is also known to be the TD error,  $\delta$ , both gradients are nonlinearly related to  $\delta$  as the nonlinear TD error,  $f(\delta) := \beta^{-1}(e^{\beta\delta} - 1)$ . Due to the positive  $\beta$ ,  $df(\delta)/d\delta \geq 0$  and  $d^2f(\delta)/d\delta^2 \geq 0$  hold: i.e.  $f(\delta)$  is the monotonically increasing convex function w.r.t.  $\delta$ . In other words, the update amount of  $\delta > 0$  is larger than that of  $\delta < 0$ , making RL optimistic.

### 3 Derivation of pessimism

#### 3.1 Inversion of optimality definition

The derivation of the above optimistic RL starts from the definition of  $p(O)$ . Remarkably, the exponential function in it is carried over to the approximated gradients, which yield the optimism. With this in mind, this paper rethinks the definition of  $p(O)$  in order to theoretically formulate the pessimism.

We have to notice that this definition can be assumed arbitrarily, except that  $p(O = 1)$  is monotonically increasing with respect to the return. Among the several possible definitions, this paper takes the following definition as a starting point, expecting that the pessimism, which is the inversion of the optimism, would emerge from the inversion of the definition in which the optimism emerged (see Fig. 2).

$$p(O = 0 \mid s) = e^{\beta(-V(s)+\underline{R})} \quad (10)$$

$$p(O = 0 \mid s, a) = e^{\beta(-Q(s,a)+\underline{R})} \quad (11)$$

where  $\beta \in \mathbb{R}_+$  denotes the inverse temperature parameter as well as the original definition.  $\underline{R}$  is the implicit minimum return to satisfy  $p(O = 0) \in (0, 1)$ . That is, as the return increases, the probability of  $O = 0$  (i.e. the future is non-optimal) monotonically decreases, and simultaneously, the probability of  $O = 1$  monotonically increases.

With this definition, the optimal and non-optimal policies are again inferred as follows:

$$\begin{aligned} \pi^+(a \mid s) &= \frac{1 - e^{\beta(-Q(s,a)+\underline{R})}}{1 - e^{\beta(-V(s)+\underline{R})}} b(a \mid s) \\ \pi^-(a \mid s) &= \frac{e^{\beta(-Q(s,a)+\underline{R})}}{e^{\beta(-V(s)+\underline{R})}} b(a \mid s) \end{aligned} \quad (12)$$

### 3.2 Derivation of pessimism

Under the new definition above, let's consider solving eqs. (6) and (7). The almost same procedure as in the case of the above optimistic RL is conducted to derive the approximated gradients.

Specifically,  $g_\theta^{\text{pessim}}$ , the gradient for  $\theta$  in the value function  $V$ , is first derived as follows:

$$\begin{aligned} g_\theta^{\text{pessim}} &= -p(O = 1 \mid s, a) \nabla_\theta \ln p(O = 1 \mid s) \\ &\quad - p(O = 0 \mid s, a) \nabla_\theta \ln p(O = 0 \mid s) \\ &= -(1 - e^{\beta(-Q(s,a)+\underline{R})}) \frac{e^{\beta(-V(s)+\underline{R})} \beta \nabla_\theta V(s)}{1 - e^{\beta(-V(s)+\underline{R})}} \\ &\quad + e^{\beta(-Q(s,a)+\underline{R})} \beta \nabla_\theta V(s) \\ &= \beta \nabla_\theta V(s) \frac{e^{\beta(-Q(s,a)+\underline{R})} - e^{\beta(-V(s)+\underline{R})}}{1 - e^{\beta(-V(s)+\underline{R})}} \\ &\propto \nabla_\theta V(s) \beta^{-1} \left( \frac{e^{\beta(-Q(s,a)+\underline{R})}}{e^{\beta(-V(s)+\underline{R})}} - 1 \right) \\ &\simeq \nabla_\theta V(s) \beta^{-1} (e^{-\beta(r+\gamma V(s')-V(s))} - 1) \end{aligned} \quad (13)$$

where the proportion is obtained by dividing the third line by  $\beta^2 e^{\beta(-V(s)+\underline{R})} (1 - e^{\beta(-V(s)+\underline{R})})^{-1} > 0$ , and  $Q(s, a)$  is finally approximated as  $r + \gamma V(s')$ . Note that for simplicity, only the inside of the expectation operation  $\mathbb{E}_{p_{e,b}[\cdot]}$  is considered here.

Similarly,  $g_\phi^{\text{pessim}}$ , the gradient for  $\phi$  in the policy  $\pi$ , is approximately derived. Again, only the inside of

the expectation operation  $\mathbb{E}_{p_e}[\cdot]$  is considered for simplicity.

$$\begin{aligned}
g_\phi^{\text{pessim}} &= \mathbb{E}_b \left[ -\frac{1 - e^{\beta(-Q(s,a)+\underline{R})}}{1 - e^{\beta(-V(s)+\underline{R})}} \nabla_\phi \ln \pi(a | s) \right. \\
&\quad \left. + \frac{e^{\beta(-Q(s,a)+\underline{R})}}{e^{\beta(-V(s)+\underline{R})}} \nabla_\phi \ln \pi(a | s) \right] \\
&= \mathbb{E}_b \left[ \frac{\nabla_\phi \ln \pi(a | s) e^{\beta(-Q(s,a)+\underline{R})} - e^{\beta(-V(s)+\underline{R})}}{e^{\beta(-V(s)+\underline{R})} (1 - e^{\beta(-V(s)+\underline{R})})} \right] \\
&\propto \mathbb{E}_b \left[ \nabla_\phi \ln \pi(a | s) \beta^{-1} \left( \frac{e^{\beta(-Q(s,a)+\underline{R})}}{e^{\beta(-V(s)+\underline{R})}} - 1 \right) \right] \\
&\simeq \mathbb{E}_b \left[ \nabla_\theta V(s) \beta^{-1} (e^{-\beta(r+\gamma V(s')-V(s))} - 1) \right] \tag{14}
\end{aligned}$$

where the proportion is given by dividing the second line by  $\beta(1 - e^{\beta(-V(s)+\underline{R})})^{-1} > 0$ . The two gradients obtained are summarized below.

$$g_\theta^{\text{pessim}} = \mathbb{E}_{p_e,b}[-\beta^{-1}(1 - e^{-\beta(r+\gamma V(s')-V(s))}) \nabla_\theta V(s)] \tag{15}$$

$$g_\phi^{\text{pessim}} = \mathbb{E}_{p_e,b}[-\beta^{-1}(1 - e^{-\beta(r+\gamma V(s')-V(s))}) \nabla_\phi \ln \pi(a | s)] \tag{16}$$

With  $f(\delta) := \beta^{-1}(1 - e^{-\beta\delta})$ ,  $df(\delta)/d\delta \geq 0$  and  $d^2f(\delta)/d\delta^2 \leq 0$  hold: i.e.  $f(\delta)$  is the monotonically increasing concave function w.r.t.  $\delta$ . In other words, the update amount of  $\delta > 0$  is smaller than that of  $\delta < 0$ , making RL pessimistic.

Compared to eqs. (8) and (9), these two equations look similar. In fact, without loss of generality, if a minus sign is included into  $\beta$  (i.e.  $\beta < 0$  is assumed), they can be expressed in exactly the same way. That is, the optimistic and pessimistic update rules can be adapted by  $\beta \in \mathbb{R}$ , as defined in the following equation and illustrated in Fig. 3.

$$f_\beta(\delta) := \begin{cases} \delta & \beta = 0 \\ \beta^{-1}(e^{\beta\delta} - 1) & \beta \neq 0 \end{cases} \tag{17}$$

$$g_\theta = \mathbb{E}_{p_e,b}[-f_\beta(\delta) \nabla_\theta V(s)] \tag{18}$$

$$g_\phi = \mathbb{E}_{p_e,b}[-f_\beta(\delta) \nabla_\phi \ln \pi(a | s)] \tag{19}$$

Note that the limits  $\beta$  to 0 from both positive and negative sides converge to  $\beta^{-1}(e^{\beta\delta} - 1) \rightarrow \delta$ . Therefore,  $f_{\beta=0}(\delta) = \delta$  is given. In addition, as can be easily seen in the figure, when  $\delta = 0$ ,  $f_\beta(0) = 0$  and  $df_\beta(0)/d\delta = 1$  hold for any  $\beta$ , yielding  $f_{\beta_1}(\delta) \geq f_{\beta_2}(\delta)$  with  $\beta_1 > \beta_2$ . In other words,  $f_\beta(\delta) - \delta \geq 0$  holds for  $\beta > 0$ , and  $f_\beta(\delta) - \delta \leq 0$  for  $\beta < 0$ .

## 4 Implementation of DROP

### 4.1 Distributional value function with ensemble model

As suggested in the literature [18], the optimistic and pessimistic update rules for the value function would achieve the ones biased positively and negatively, respectively. By combining the value functions learned with the optimistic-to-pessimistic update rules, the distributional value function can be modeled implicitly, although errors might occur compared to learning an explicit distribution [21]. This might improve the accuracy of value estimation and also allows for applications such as a risk-sensitive optimization like [30], although they are out of the scope in this paper.

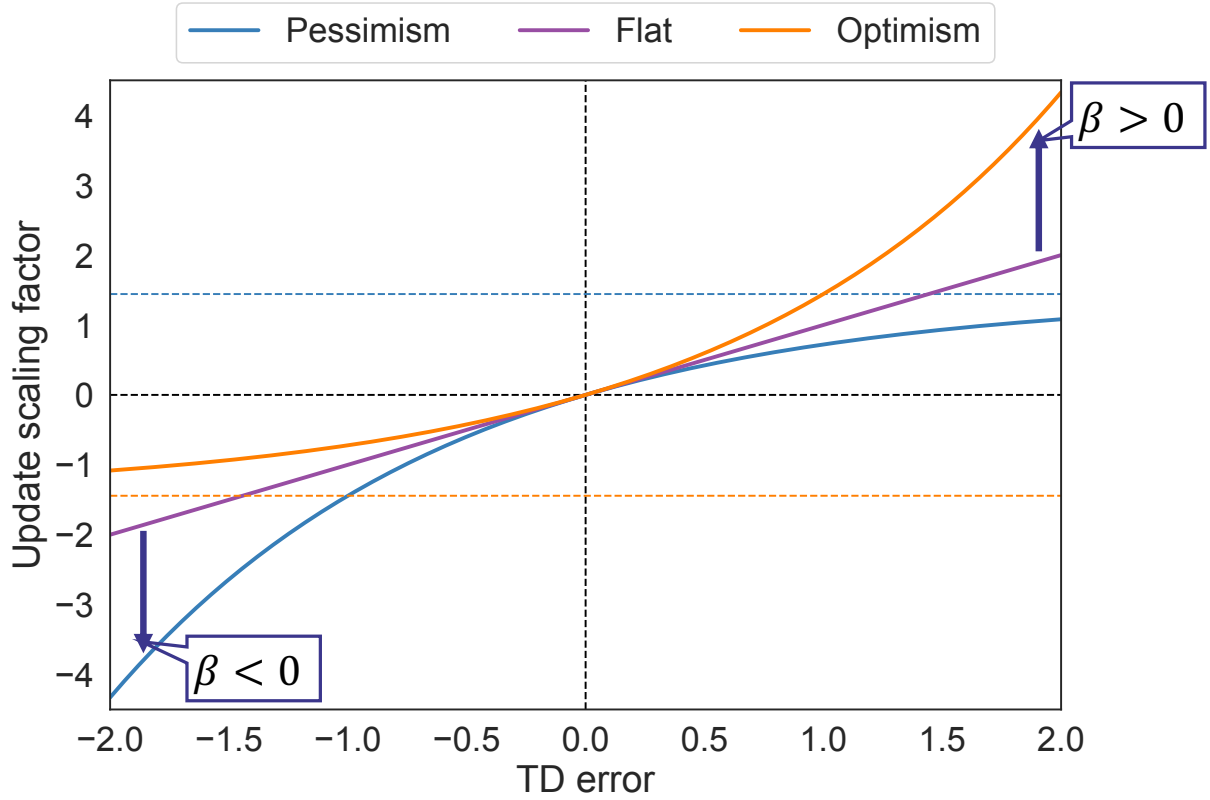


Figure 3: Optimistic and pessimistic TD errors parameterized by  $\beta \in \mathbb{R}$ : when  $\beta > 0$ , the update scale is positively biased with optimism from the original TD error; symmetrically, pessimism can be obtained with  $\beta < 0$ .

Specifically, eq. (18) is extended to the distributional version simply with an ensemble model of  $N$  estimates of  $V$  with the respective parameters  $\boldsymbol{\theta} = [\theta_1, \theta_2, \dots, \theta_N]$ . These are separately optimized with the different inverse temperature parameters,  $\boldsymbol{\beta} = [\beta_1, \beta_2, \dots, \beta_N]$ , as follows:

$$\begin{aligned}\theta_i &\leftarrow \theta_i - \alpha \mathbb{E}_{(s,a,s',r) \sim \mathcal{D}} [-f_{\beta_i}(\delta_i) \nabla_{\theta_i} V_i(s)] \\ \delta_i &= r + \gamma V_i(s') - V_i(s)\end{aligned}\quad (20)$$

where  $\alpha \in \mathbb{R}_+$  denotes the learning rate and  $\mathcal{D}$  is the replay buffer storing the experience data in a FIFO manner. As a remark, this ensemble model is implemented with a shared model before outputs and  $N$  separated linear mappings for reducing its computational complexity (see Fig. 4). Note that although the previous studies [18, 19] sample one value function for  $s'$  to compute all the TD errors, this paper employs the local version, which computes the above update in each cell independently, according to biological feasibility pointed out in the literature [21].

Next,  $\boldsymbol{\beta}$  is designed regularly. Unfortunately,  $\beta_i \in \mathbb{R}$  makes their balanced placement difficult. The effective range of  $\beta_i$  would be implicitly affected by the scale of the TD error.

To resolve these issues, the upper or lower bound of  $f(\delta)$  is utilized based on the previous work [27]: with  $\eta, \beta > 0$ , the lower bound is given as  $-\beta^{-1}$ ; and with  $\eta, \beta < 0$ , there is the upper bound on  $-\beta^{-1}$  as well. Note that the previous work only considered the lower bound as  $\beta$  was limited to be positive. Under such boundaries, another parameter  $\eta \in (-1, 1)$ , which is invertible with  $\beta$ , is defined as the ratio between either of them and the value at the empirical worst-case TD error,  $\pm|\bar{\delta}|$ . Specifically,  $\beta_i$  is invertibly mapped from  $\eta_i$  as follows:

$$\beta_i = -\frac{\text{sgn}(\eta_i)}{|\bar{\delta}|_i} \ln(1 - |\eta_i|) \quad (21)$$

where  $\text{sgn}(\cdot)$  denotes the sign function, and therefore,  $\eta = 0$  gets  $\beta = 0$ . As  $|\bar{\delta}|$  is in the denominator, the scale issue is resolved. In addition, as  $\eta$  is in  $(-1, 1)$ ,  $\boldsymbol{\eta} = [\eta_1, \eta_2, \dots, \eta_N]$  can be regularly placed.

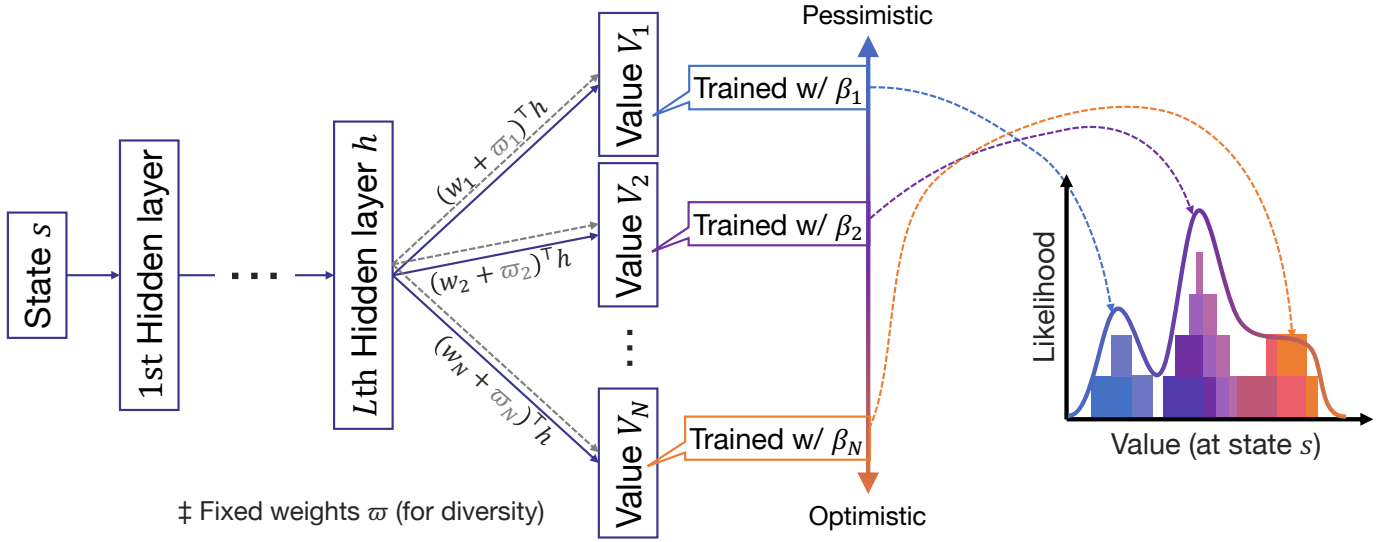


Figure 4: Distributional value function modeled by an ensemble model of multiple value functions with different optimism/pessimism: the network parameters before the output layer are all shared between  $N$  value functions; with randomly fixed weights for diversity, the output layer separately estimates the respective value functions, which are trained with the corresponding  $\beta_1, \dots, \beta_N$ ; as value functions trained with biased TD errors are biased as well, their ensemble can represent the distribution of value functions.

## 4.2 Policy improvement with central value

Since this algorithm estimates multiple value functions,  $\mathbf{V} = [V_1, V_2, \dots, V_N]$ , it can be interpreted as a kind of multi-objective RL [31, 32]. Accordingly, two approaches are raised for acquiring the optimal policy: one is to optimize a single policy with the scalarized  $\mathbf{V}$ ; and another is to build a mixture distribution, the components of which are optimized with the corresponding value functions. The former makes the learning cost minimal while its policy depends on the way of scalarization and has no adaptability after learning. The latter needs the  $N$ -times learning cost while its policy can be fine-tuned by adjusting its mixture ratio. This paper does not focus on the way of fully exploiting the distributional value function, so for simplicity, the former is employed.

Specifically, from  $\mathbf{V}$  and  $\beta$ , the respective nonlinear TD error,  $f_\beta(\delta) = [f_{\beta_1}(\delta_1), f_{\beta_2}(\delta_2), \dots, f_{\beta_N}(\delta_N)]$ , are computed. The central value of  $f_\beta(\delta)$  is extracted using  $\mathcal{M} : \mathbb{R}^N \rightarrow \mathbb{R}$ , which replaces  $f(\delta)$  in eq. (19).

That is, the update rule of  $\phi$  can be renewed as follows:

$$\begin{cases} \phi & \leftarrow \phi - \alpha \mathbb{E}_{(s,a,s',r) \sim \mathcal{D}} [-\mathcal{M}(f_\beta(\delta)) \nabla_\phi \ln \pi(a | s)] \\ \mathcal{M}(f_\beta(\delta)) & \stackrel{\text{e.g.}}{=} \text{Median}(f_\beta(\delta)) \end{cases} \quad (22)$$

where the median operation is employed as the central value since it is robust to outliers in  $f_\beta(\delta)$ , making the policy improvement stable (see Fig. 5).

As a remark, in a prioritized experience replay (PER) [33], the absolute value of the (nonlinear) TD error is utilized for computing the priority of each experience data.  $f_\beta(\delta)$  cannot be utilized for that purpose since the priority must be scalar, although the nonlinear TD error makes sampling optimistic or pessimistic. Instead, the absolute value of  $\mathcal{M}(f_\beta(\delta))$  is employed.

## 5 Simulations

### 5.1 Conditions

#### 5.1.1 Task

The proposed method, DROP, is verified on the learning performance of a total of six tasks. Specifically, Hopper, HalfCheetah, and Ant implemented respectively on Mujoco [28] and Pybullet [29] are employed



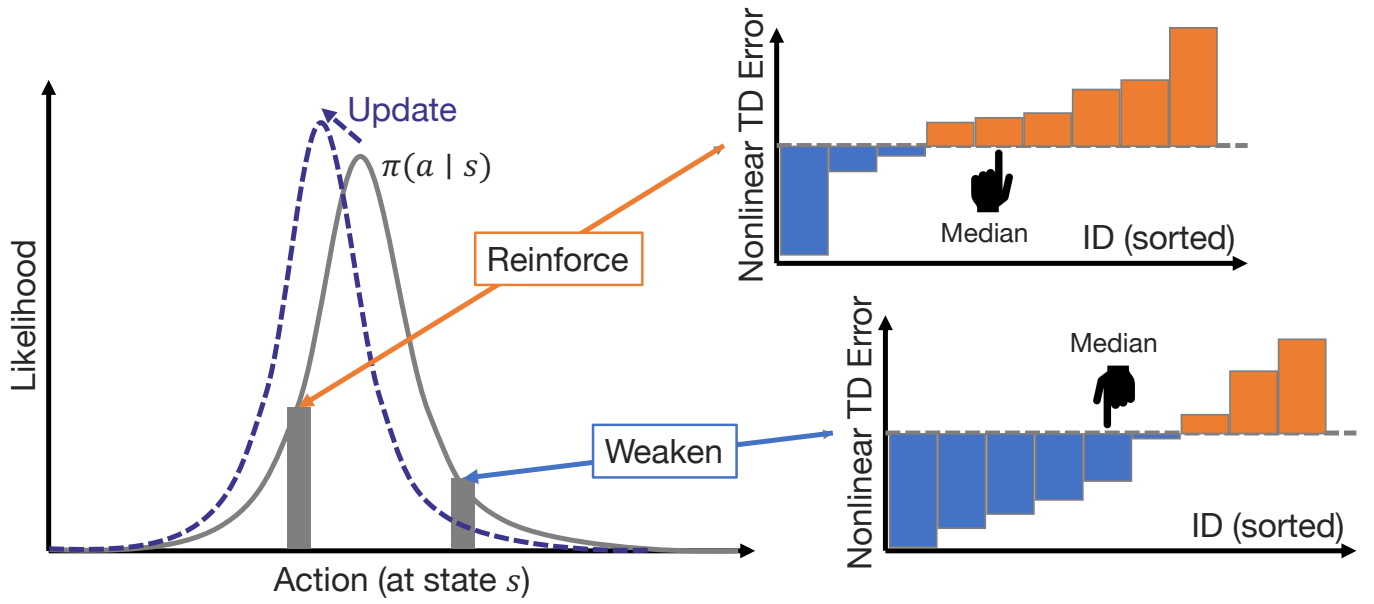


Figure 5: Policy improvement with ensemble of optimistic/pessimistic value functions: since learning multiple policies is costly, a single policy is optimized based on a central value of nonlinear TD errors calculated from multiple value functions; by employing the median as this central value, the direction of the policy improvement can be properly determined without being affected by outliers.

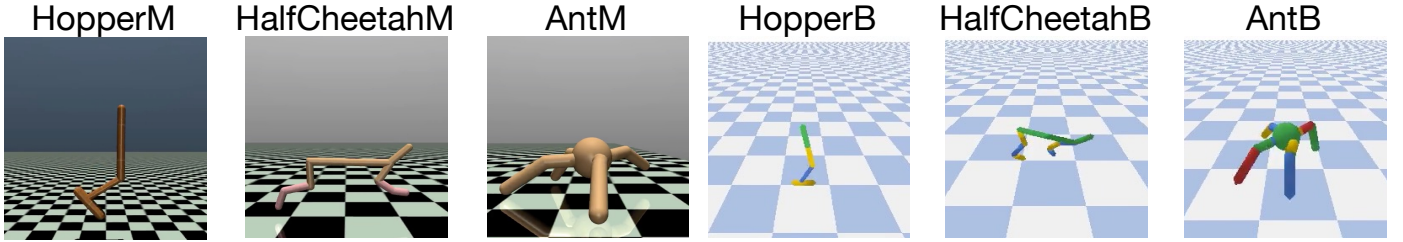


Figure 6: Benchmark tasks to be conducted in this paper: Mujoco [28] and Pybullet [29] for simulating three tasks are distinguished with ‘M’ and ‘B’ on the suffix of each task, respectively; it should be noticed that in these two simulators, the dynamics, models and reward functions are different.

as the tasks, as shown in Fig. 6. Here, ‘M’ for Mujoco and ‘B’ for Pybullet are added to the suffix of each task name to distinguish between them. The reason why two simulators are tested is that their dynamics computation, models used (especially their maximum torques), and reward functions are different, resulting in different learning tendencies. Note that there are several versions of task implementation on Mujoco, but v4 is used in this paper. In addition, the OpenAI Gym API is used, and unlike the new API in Gymnasium, when a task is terminated due to a time limit, it is treated in the same way as an end condition defined for the task.

All tasks are terminated in the number of episodes rather than in the number of data experienced, with 2000 episodes being the upper limit in this paper. The learning performance (or score) is evaluated by the statistic (i.e. the interquartile mean referring to the literature [34]) of the returns obtained by 100 episodes with the optimized policy. The 12 models for each method are initialized with different seeds and trained in the same way. Then, the proposed and baseline methods are compared statistically.

### 5.1.2 Heuristic model with asymmetric learning rates

In the heuristic model proposed in the previous studies [18, 19], the learning rate  $\alpha$  itself is switched by the positive or negative TD error, as  $\alpha^{+,-}$ , as illustrated in Fig. 1. This implementation differs from DROP, making a fair comparison difficult. This paper, therefore, modifies it slightly to include a learn-

Table 1: Learning conditions: the methods combined in the proposed algorithm use the default hyperparameters given in the references presented, unless otherwise noted.

#Hidden layers of fully connected networks	2
#Neurons for each hidden layer	100
Activation function	Squish [37, 38] + RMSNorm [39]
Estimation model of each value function	Ensemble model [40]
Distribution model of policy	Student's t-distribution [13]
Discount factor $\gamma$	0.99
Optimizer	AdaTerm [36]
The way of updating target networks	CAT-soft update [41]
Stabilization tricks	L2C2 [42] + ERC [35]
Buffer size $ \mathcal{D} $	102400
Batch size	32
#Replayed data	$ \mathcal{D} /8$
Hyperparameters of PER [33] ( $\alpha^{\text{PER}}, \beta^{\text{PER}}$ )	(1, 0.5)

ing rate multiplier (i.e.  $\alpha^{+,-}/\alpha$ ) in  $f(\delta)$ , in line with this study.

$$f_{\eta}^{\text{heuristic}}(\delta) = (1 + \text{sgn}(\delta)\eta)\delta \quad (23)$$

where  $\eta \in (-1, 1)$  is the optimistic/pessimistic hyperparameter as well as that of DROP. That is, with  $\eta \rightarrow 1$ ,  $\delta < 0$  is ignored for optimistically updating  $\theta$  (and  $\phi$ ); and with  $\eta \rightarrow -1$ , the perfect pessimism is obtained by ignoring  $\delta > 0$ .

### 5.1.3 Learning

To stabilize RL, ERC [35] is employed in conjunction with DROP. Therefore, the learning conditions including the network architecture are basically based on the implementations in that literature. For example, by using AdaTerm [36] with its default setting (e.g.  $\alpha = 10^{-3}$ ) as an optimizer, the network parameters,  $\theta$  and  $\phi$ , are learned robustly to the noise of (nonlinear) TD errors.

However, the use of the replay buffer is changed from the usual uniform sampling to PER [33] because the use of PER can emphasize optimism (and pessimism in this study), as indicated in the previous work [27]. In that case, the buffer size is set to 32 and the number of experiences to be replayed at the end of the episode is set to 1/8 of the buffered data (a maximum size of 102400). In addition, as for the number of ensembles,  $N$ , and the range of optimism and pessimism,  $\eta$ , in the critic, they are additional elements that appeared in this study and are tuned as shown in the next section.

The overall learning conditions are summarized in Table 1. Note that hyperparameters used in the combined methods are left at their default settings unless otherwise explained.

## 5.2 Results

### 5.2.1 Parameter tuning

First, the number of ensembles,  $N$ , is tuned by a gridsearch. Here, the maximum of  $\eta$  is tentatively set to a moderate 0.5 as suggested by the previous study [27], and the minimum is set to  $-0.5$  as well. Then,  $\eta$  is regularly placed according to  $N = 3, 4, \dots, 10$  using a linspace function.

The score of each task is normalized to  $[0, 1]$ , and in order to consider generality to tasks, it is divided by the gap between the maximum and minimum scores in each condition. As shown in Fig. 7a, the best score was obtained for  $N = 9$ . Although the trend seems to be that the score improves with larger  $N$ , the score with  $N = 10$  was suddenly deteriorated. This may be due to the fact that the ensemble model was not implemented in independent networks but was partially shared, as shown in Fig. 4, resulting in a lack of expressiveness. This is also consistent with the fact that the slight improvement in performance at  $N = 3$ , probably due to the extra expressiveness.

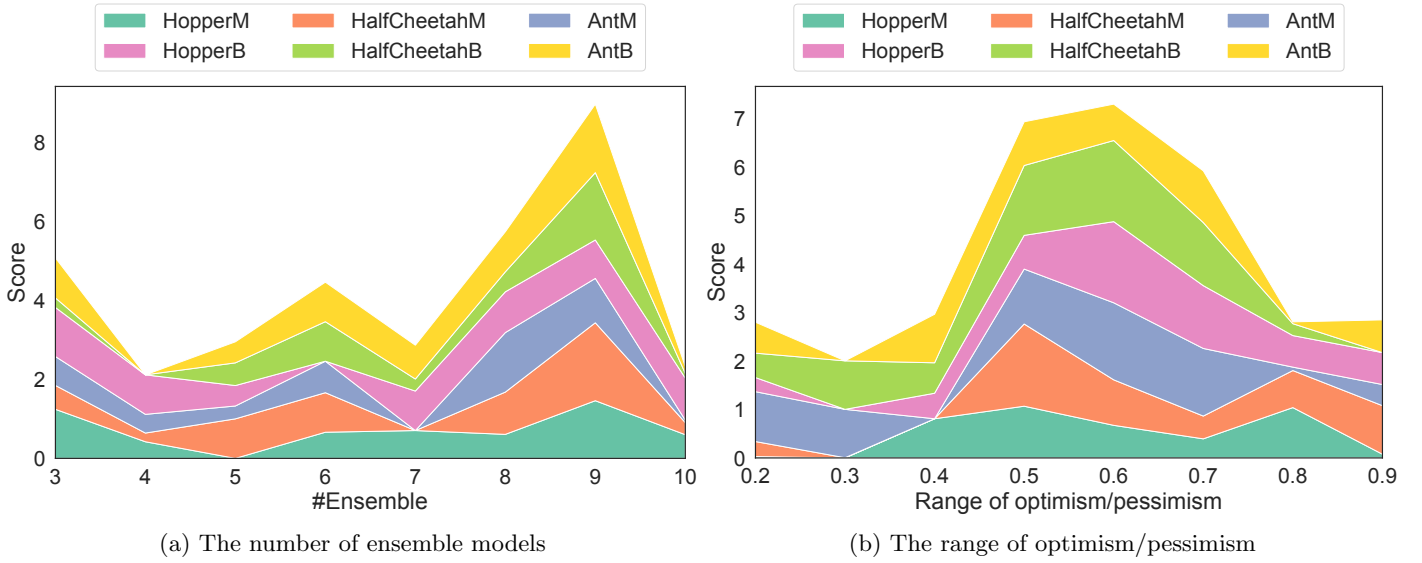


Figure 7: Parameter tuning in DROP: the score for each score is computed as the interquartile mean of 12 random seeds and normalized; the scores for each condition are divided by the gap between their maximum and minimum in order to consider generality to tasks; as a result,  $N = 9$  and  $\eta_i \in [-0.6, 0.6]$  obtained the best score.

Next, the maximum and minimum values of  $\boldsymbol{\eta}$ ,  $\pm\bar{\eta}$ , are tuned by a gridsearch along with the tuned  $N = 9$ .  $\bar{\eta} = 0.2, 0.3, \dots, 0.9$  with 0.1 increments are compared as in the case of  $N$ . The scores are shown in Fig. 7b, where  $\bar{\eta} = 0.6$  is the best one. This result is consistent with the previous study, which showed that a moderate level of optimism (and pessimism) is superior to the others.

### 5.2.2 Comparison

From the parameter tuning conducted above,  $\boldsymbol{\eta} = [-0.6, -0.45, -0.3, -0.15, 0, 0.15, 0.3, 0.45, 0.6]$  with  $N = 9$  is used for the proposed DROP. As well, the heuristic model defined in eq. (23) employs the same setting for comparison. With three additional ablation tests, the following five methods are compared in total.

- *Flat*: with  $\boldsymbol{\eta} = [0]$  as a non-biased traditional RL
- *Optim*: with  $\boldsymbol{\eta} = [0.6]$  as an optimistic RL derived in the previous study [27]
- *Pessim*: with  $\boldsymbol{\eta} = [-0.6]$  as a pessimistic RL derived in this paper
- *Heuristic*: with the tuned parameters and the replacement of eq. (17) with eq. (23) as a heuristic model in the literature [18, 19]
- *Proposal*: with the tuned parameters as the proposed DROP

The scores are summarized in Fig. 8. Note that the corresponding 95 % confidence intervals are provided for reference, since the scores vary greatly depending on the success or failure of the task and are bimodal.

First, *Flat*, *Optim*, and *Pessim* excelled at different tasks. For example, *Optim* with better exploration capability was superior for HalfCheetahB, which tends to stay in a local solution of standing due to insufficient torques, while *Pessim* with better safety capability and *Flat* were superior for AntM, which is prone to fall over and gain unworthy experience due to excessive torques. In the latter case, the reason why *Flat* was also superior is probably due to the fact that the recent RL stabilization tricks (e.g. the ones used in this paper as summarized in Table 1) is to make learning proceed conservatively, i.e. pessimistically. This reason is also reasonable for explaining the reason why *Pessim* was not good in the other tasks, namely, the overlapping effects prevented the sufficient exploration for finding a global optimum.

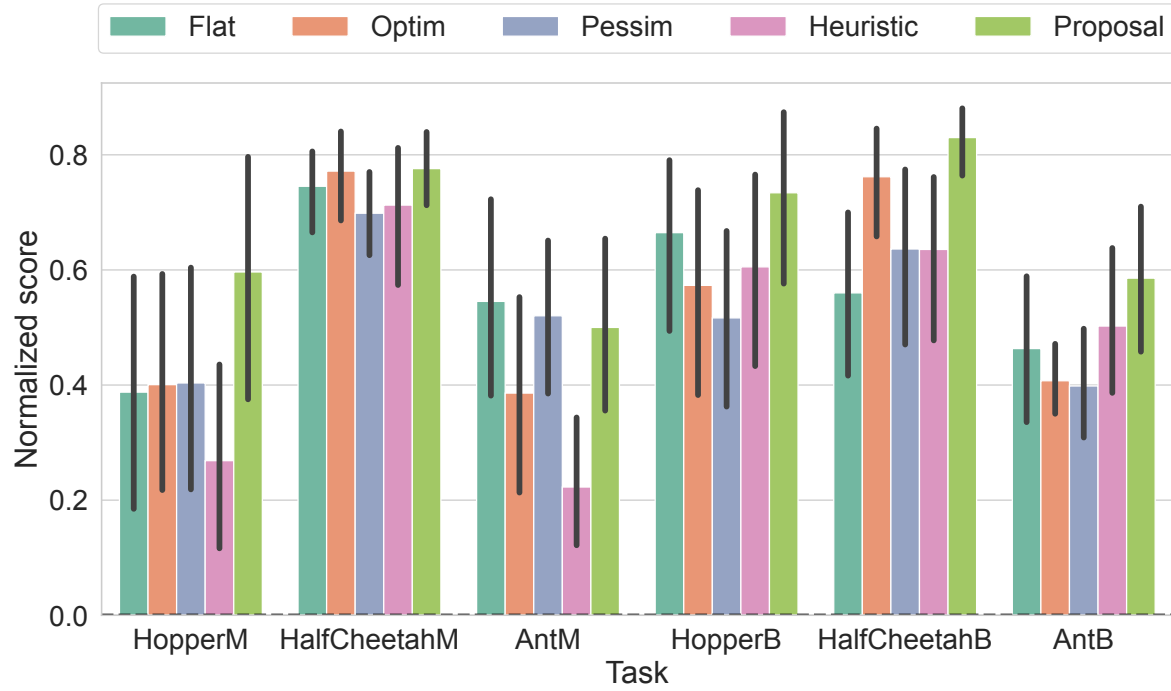


Figure 8: Comparison of five methods: the first three methods, *Flat*, *Optim*, and *Pessim*, represent the cases with  $\eta = 0, 0.6, -0.6$  and  $N = 1$ , respectively, *Heuristic* is based on the previous studies [ ] implemented in eq. (23), and *Proposal* means the proposed method, named DROP; only *Proposal* succeeded in all the tasks stably.

Next, the scores for *Heuristic* were generally poor. In particular, it have the worst scores on HopperM and AntM. This should be due to the discontinuous TD error near  $\delta \simeq 0$ , destabilizing its learning. In fact, looking at the learning curve w.r.t. the TD error scale in Fig. 9, only *Heuristic* was not able to make the TD error converge to almost zero. In addition, as suggested in Fig. 10 for the averaged optimistic/pessimistic bias computed as  $f(\delta) - \delta$ , the pessimistic learning of the value function was unsuccessful, as it was biased negatively. Note that *Proposal* kept the bias zero, implying both the optimistic and pessimistic value functions were trained to the same level.

On the other hand, only *Proposal* achieved high-quality behaviors in all tasks, namely, it outperformed or was comparable to scores of the other methods. In fact, when the behaviors at the average scores were checked, as shown in the attached video, only its behaviors could be considered qualitatively successful in all tasks. In addition, the learnings curve w.r.t. the returns are depicted in Fig. 11, indicating that it learned the optimal policies earlier than the other methods.

While the hyperparameters tuned with DROP in the above section may be one possible factor of this superiority in *Proposal*, it cannot be the reason for collapsing the learning of *Heuristic*, which is the main

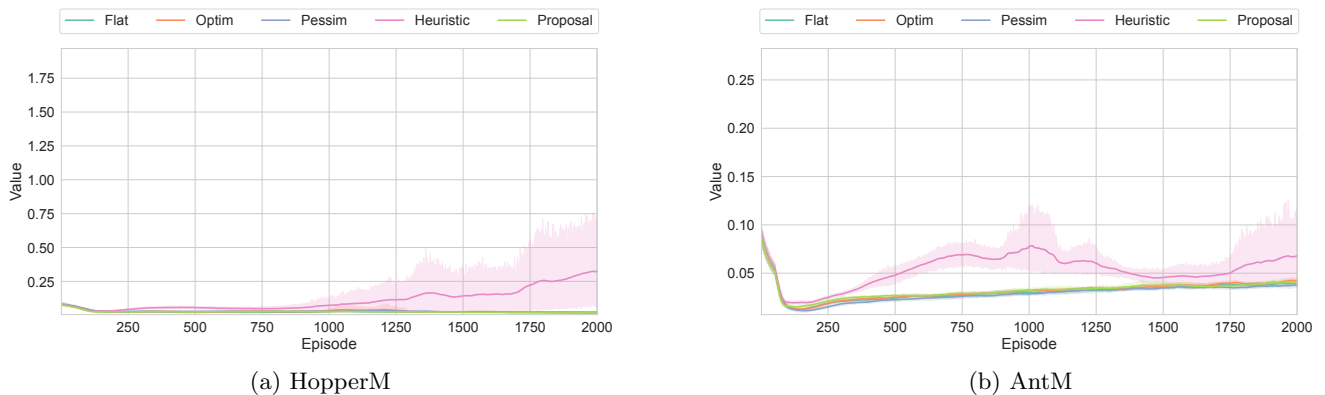


Figure 9: The averaged scale of TD errors during learning: only *Heuristic* failed the convergence of TD error in these tasks, collapsing the policy as can be seen in Fig. 8.

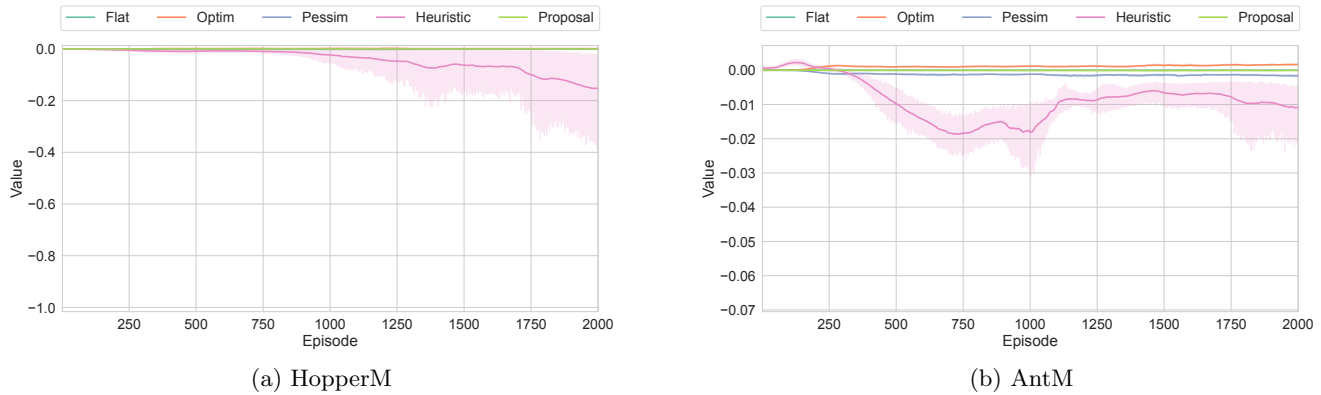


Figure 10: The averaged optimistic/pessimistic bias during learning: in *Heuristic*, the TD error for the pessimistic value function was not minimized appropriately since the bias diverged negatively; such a bias was not observed in *Proposal* by canceling out the small biases in the optimistic and pessimistic value functions.

baseline for comparison. The design by eq. (23) of the heuristic model is also not much different in terms of the ratio of positive and negative updates: for the  $\eta$  used in this paper, 4 : 1 at most in the heuristic model, while DROP defined by eqs. (17) and (21) has the similar ratio, 5 : 2, when  $\delta = \pm|\bar{\delta}|$ . Note that  $|\bar{\delta}|$  is the empirically estimated maximum scale, so the actual TD error can cause  $\delta > |\bar{\delta}|$  (or  $\delta < -|\bar{\delta}|$ ), making the ratio larger. Thus, it can be concluded that the theoretically-grounded DROP performed better than the heuristic model.

## 6 Conclusion and future work

This paper investigated a novel theoretically-grounded model of RL derived on the basis of the control as inference, which replaces the heuristic model with asymmetric learning rates to explain the real behaviors of dopamine neurons reported in the recent studies [18, 19]. First, the derivation of optimistic model in the previous study [27] was reviewed, and then, a pessimistic model was theoretically derived by considering the inversion of the definition of optimality. Then, the degree of optimism and pessimism was made adjustable with a single bounded parameter, and both optimism and pessimism were obtained in a balanced manner by regularly spacing multiple parameters based on an ensemble method. While the heuristic model sometimes failed in learning, the proposed method, DROP, could succeed in stable learning with appropriately small TD errors.

Thus, the heuristic model used to explain the real data was not useful as a RL algorithm, but DROP was useful as it, partly because it was theoretically grounded. Conversely, using DROP to explain real data may enable fitting with higher accuracy than the heuristic model. Therefore, it would be worthwhile to use DROP as a model to explain the real data.

On the other hand, there is still room for improvement in DROP as a RL algorithm. Specifically, DROP can make effective use of the distributional value function, which is omitted in this paper for simplicity. Depending on how it is used, DROP should be effective in various ways, such as ensuring safety through worst-case optimization, efficient exploration prioritizing the best-case scenario, and so on. Alternatively, it would be interesting to see if the consideration and introduction of biologically-plausible meta-objective, which optimizes the statistic  $\mathcal{M}$ , can also explain the policy improvement in animals.

### Supporting Information

Supporting Information is available from the Wiley Online Library or from the author.

### Acknowledgements

This work was supported by JSPS KAKENHI, Development and validation of a unified theory of prediction and action, Grant Number JP24H02176.

### Conflict of Interest

The author declare no potential conflict of interests.

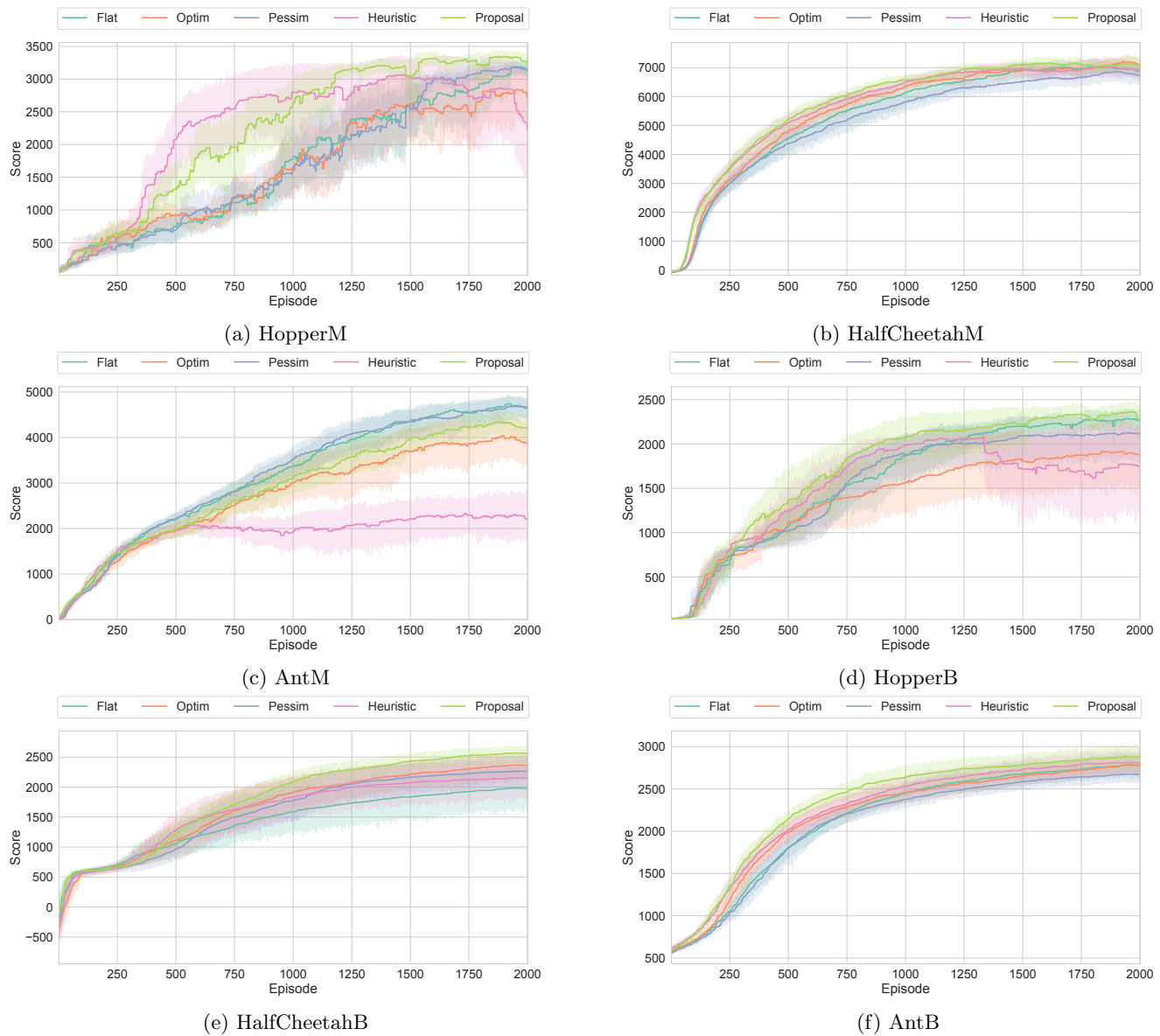


Figure 11: Learning curves of return: *Heuristic* was unstable even if it increased the return rapidly, collapsing the policy suddenly; *Proposal* was faster and more stable than others in most tasks.

## References

- [1] R. S. Sutton, A. G. Barto, *Reinforcement learning: An introduction*, MIT press, **2018**.
- [2] P. Wu, A. Escontrela, D. Hafner, P. Abbeel, K. Goldberg, In *Conference on Robot Learning*. PMLR, **2023** 2226–2240.
- [3] I. Oh, S. Rho, S. Moon, S. Son, H. Lee, J. Chung, *IEEE Transactions on Games* **2021**, 14, 2 212.
- [4] Y. Cui, S. Osaki, T. Matsubara, *Journal of Field Robotics* **2021**, 38, 3 331.
- [5] W. Schultz, P. Apicella, T. Ljungberg, *Journal of neuroscience* **1993**, 13, 3 900.
- [6] C. K. Starkweather, N. Uchida, *Current Opinion in Neurobiology* **2021**, 67 95.
- [7] S. C. Tanaka, N. Schweighofer, S. Asahi, K. Shishida, Y. Okamoto, S. Yamawaki, K. Doya, *PloS one* **2007**, 2, 12 e1333.
- [8] R. S. Koolschijn, B. Polner, J. M. Hoomans, R. Cools, E. Vassena, H. E. den Ouden, *Current Opinion in Behavioral Sciences* **2024**, 60 101453.

- [9] B. Blain, T. Sharot, *Current Opinion in Behavioral Sciences* **2021**, *39* 113.
- [10] G. Molinaro, A. G. Collins, *PLoS Biology* **2023**, *21*, 7 e3002201.
- [11] S. Levine, *arXiv preprint arXiv:1805.00909* **2018**.
- [12] K. Doya, *Current Opinion in Behavioral Sciences* **2021**, *41* 160.
- [13] T. Kobayashi, *Applied Intelligence* **2019**, *49*, 12 4335.
- [14] X. Wang, D. Li, *Neurocomputing* **2024**, *574* 127291.
- [15] T. Kobayashi, T. Aotani, J. R. Guadarrama-Olvera, E. Dean-Leon, G. Cheng, In *Joint IEEE International Conference on Development and Learning and Epigenetic Robotics*. IEEE, **2019** 37–42.
- [16] J. Wang, S. Elfving, E. Uchibe, *Neural Networks* **2021**, *135* 115.
- [17] D. Ha, J. Schmidhuber, *arXiv preprint arXiv:1803.10122* **2018**.
- [18] W. Dabney, Z. Kurth-Nelson, N. Uchida, C. K. Starkweather, D. Hassabis, R. Munos, M. Botvinick, *Nature* **2020**, *577*, 7792 671.
- [19] T. H. Muller, J. L. Butler, S. Veselic, B. Miranda, J. D. Wallis, P. Dayan, T. E. Behrens, Z. Kurth-Nelson, S. W. Kennerley, *Nature Neuroscience* **2024**, *27*, 3 403.
- [20] M. G. Bellemare, W. Dabney, R. Munos, In *International conference on machine learning*. PMLR, **2017** 449–458.
- [21] P. Tano, P. Dayan, A. Pouget, *Advances in neural information processing systems* **2020**, *33* 13662.
- [22] K. Ciosek, Q. Vuong, R. Loftin, K. Hofmann, *Advances in Neural Information Processing Systems* **2019**, *32*.
- [23] A. Wachi, Y. Sui, In *International Conference on Machine Learning*. PMLR, **2020** 9797–9806.
- [24] S. Curi, I. Bogunovic, A. Krause, In *International Conference on Machine Learning*. PMLR, **2021** 2254–2264.
- [25] T. Moskovitz, J. Parker-Holder, A. Pacchiano, M. Arbel, M. Jordan, *Advances in Neural Information Processing Systems* **2021**, *34* 12849.
- [26] A. Bura, A. HasanzadeZonuzi, D. Kalathil, S. Shakkottai, J.-F. Chamberland, *Advances in neural information processing systems* **2022**, *35* 1047.
- [27] T. Kobayashi, *Neural Networks* **2022**, *152* 169.
- [28] E. Todorov, T. Erez, Y. Tassa, In *IEEE/RSJ international conference on intelligent robots and systems*. IEEE, **2012** 5026–5033.
- [29] E. Coumans, Y. Bai, *GitHub repository* **2016**.
- [30] D. Kim, S. Oh, *IEEE Robotics and Automation Letters* **2022**, *7*, 2 2621.
- [31] C. F. Hayes, R. Rădulescu, E. Bargiacchi, J. Källström, M. Macfarlane, M. Reymond, T. Verstraeten, L. M. Zintgraf, R. Dazeley, F. Heintz, et al., *Autonomous Agents and Multi-Agent Systems* **2022**, *36*, 1 26.
- [32] W. E. L. Ilboudo, T. Kobayashi, T. Matsubara, In *IEEE/RSJ International Conference on Intelligent Robots and Systems*. IEEE, **2023** 5622–5629.
- [33] T. Schaul, J. Quan, I. Antonoglou, D. Silver, In *International Conference on Learning Representations*. **2016** .

- [34] R. Agarwal, M. Schwarzer, P. S. Castro, A. C. Courville, M. Bellemare, *Advances in neural information processing systems* **2021**, *34* 29304.
- [35] T. Kobayashi, *Applied Intelligence* **2024**, *54*, 19 9381.
- [36] W. E. L. Ilboudo, T. Kobayashi, T. Matsubara, *Neurocomputing* **2023**, *557* 126692.
- [37] J. T. Barron, *arXiv preprint arXiv:2112.11687* **2021**.
- [38] T. Kobayashi, T. Aotani, *Advanced Robotics* **2023**, *37*, 12 719.
- [39] B. Zhang, R. Sennrich, *Advances in Neural Information Processing Systems* **2019**, *32* 12381.
- [40] T. Kobayashi, *Results in Control and Optimization* **2023**, *12* 100244.
- [41] T. Kobayashi, In *International Joint Conference on Neural Networks*. IEEE, **2024** 1–8.
- [42] T. Kobayashi, In *IEEE/RSJ International Conference on Intelligent Robots and Systems*. IEEE, **2022** 4032–4039.